

LAMINAR FLAME SPEEDS OF ETHANOL, *n*-HEPTANE, *ISO*-OCTANE AIR MIXTURES

HARA Takashi* and TANOUE Kimitoshi
Department of Mechanical Engineering, Oita University, Japan

KEYWORDS – Ethanol, *n*-Heptane and Iso-octane-air flames, Laminar Burning velocity

ABSTRACT – One of the most important properties of premixed flames is burning velocity. Laminar burning velocities play essential roles in determining several important aspects of the combustion process in spark ignition engines; among these are the ignition delay, the thickness of the wall quench layers, and the minimum ignition energy. It is found that a detailed knowledge of laminar premixed flames will provide insights into such properties as heat release rate, flammability limits, propagation rates, quenching and emissions characteristics. It is also common to use measured burning velocities to validate chemical kinetic schemes. The production of accurate measurements on laminar premixed flames therefore plays a key role in the process of understanding a large range of flames. Although the majority of fuel is probably burnt in turbulent combustion, data on laminar burning velocities are still needed as input to many turbulent combustion models. Also, in internal combustion engines the initial combustion is laminar, so again there is a need for the laminar burning velocity. In this study, laminar burning velocities of ethanol, *iso*-octane and *n*-heptane-air mixtures were determined experimentally over a wide range of equivalence ratio at atmospheric pressure, employing spherically expanding flames. Using linear extrapolations, the effects of stretch was minimized by extrapolating the reference flame speed to vanishing stretch. The laminar burning velocities of *iso*-octane were found to be lower than those of ethanol and *n*-heptane throughout the range of experimental equivalence ratios. The measured burning velocities were also compared with those of other researchers, suggesting there were good agreement between present data and those of other researchers. In addition, the effects of ethanol addition to *n*-heptane and *iso*-octane-air flames were investigated, suggesting that ethanol addition was found to make *n*-heptane and *iso*-octane-air flames stable for fuel rich region.

INTRODUCTION

In recent years computer simulation models of spark ignition engines have been extensively utilized as tool to understand the effects of various engine variables on exhaust emissions and fuel economy (1). Due to the complexity of many practical combustion phenomena, some of these simulations have used turbulent combustion models which require acknowledge of laminar burning velocity of the fuel-air mixture. Nowadays, even the detailed kinetic models are being used for practical engine simulations. In order to validate their accuracy and test their range of applicability, it is important that these turbulent combustion models and kinetic models be compared with experimental data of high fidelity, such as the flame structure and response. For the flame response, a widely use parameter is the laminar burning velocity that describes the propagation of the one-dimensional, planar, adiabatic, premixed flame in the doubly infinite domain. The laminar burning velocity embodies the fundamental information on the diffusivity, reactivity, and exothermicity of a given mixture and has been extensively used to partially validate proposed combustion models. If a proposed model could not reproduce the laminar burning velocity, its comprehensiveness and utility would obviously require further examination. Therefore, an accurate knowledge of laminar burning velocity,

together with the influence of other properties on it, is important in any combustion study, especially for practical fuels.

The purpose of this study is to measure the laminar burning velocities and clarify the effects of flame stretch on them for ethanol, *n*-heptane, *iso*-octane-air flames, which should be useful data for combustion modelling and simulation, using the spherical bomb that can embody the real engine conditions. Numerous experimental methods have been developed in order to measure the fundamental burning velocity of a combustible mixture, and many reviews have evaluated the different methods of determining the burning velocity. Here we used the spherical bomb to determine the laminar burning velocity. Even though there is no real agreement on a standardized method of measurement, it is generally accepted that the spherical bomb permits the determining the laminar burning velocity with best precision, 5 to 10%. The spherical bomb is said to be best suited to measuring flame speeds of average velocity ranging from 20 to 80 cm/s.

Our second objective is to investigate the effects of ethanol addition to *n*-heptane and *iso*-octane-air flames. Recently based on the environmental issues on an earth scale and the depletion of energy resources, the increasing concern with the use of alcohols as alternative fuels have stimulated extensive fundamental studies on their combustion properties (2)(3). Ethanol, being the second simplest alcohol, has been extensively studied. Growing concern about alcohol fuel utilization has also necessitated combustion properties data for studies related with engines fuelled with alcohols. One example of importance of investigating the effects of ethanol addition can be shown by the behaviour of the spark timing for the engine fuelled with ethanol (3). Spark ignition engines fuelled with ethanol require less advanced spark timing as compared to that of gasoline. On the other hand, gasoline-alcohol blends need more advanced spark timing for maximum torque output than those needed with gasoline and alcohols.

EXPERIMENTAL SETUP

The combustion chamber (4)(5) used in this study is a nearly spherical vessel with a mean inner diameter of about 100 mm and a total volume of about 2000 cm³. It is fixed with four transparent windows of 92 mm diameter at four sides for flame observation, and two perforated plates of 92 mm diameter at two opposite sides. The cross-sectional view of the combustion chamber observed from the transparent window is shown in Fig.1. Behind each perforated plate, a fan is installed to mix gases to obtain perfectly premixed mixtures.

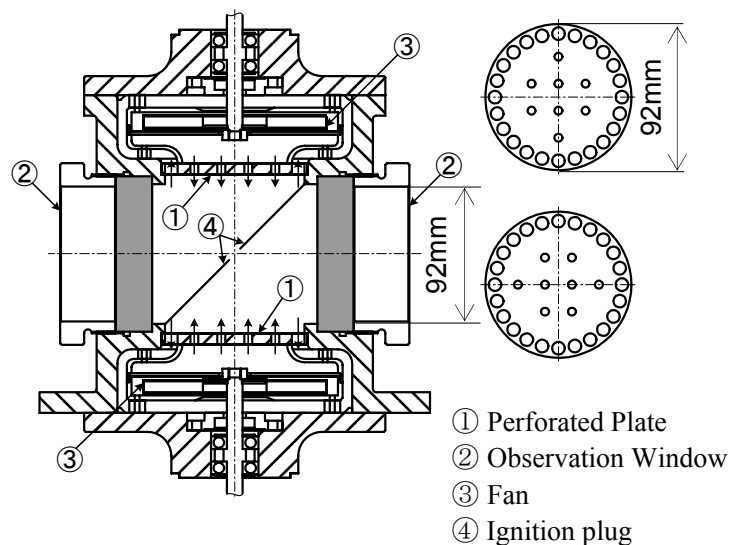


Fig.1 Combustion Chamber

The combustible mixture was spark-ignited at the center of the chamber using minimum spark ignition energies to avoid ignition disturbances. The flames were observed using schlieren system with high speed camera (1000 pictures per second). A schlieren image was recorded up to the instant where any part of it reached the edge of the viewing window in the bomb. Once combustion was complete, the chamber was vented and the flushed with air to remove condensed water vapour and to cool the system to the allowable initial temperature range of the experiment. The high-speed camera has a field-of-view of 36×34 mm at a resolution of 0.14 mm/pixel, which is estimated to be enough to resolve the flames for the flame radius ranging from 3 mm to 35 mm. For this range, pressure increases were found to be less than 0.7 % of the initial pressure. Similar to other work (4)(5), measurements were limited to $\delta r^0/r < 2$ % so that effects of curvature and transient phenomena associated with large flame thickness were small. Finally, radiative heat loss was small due to the large flame speeds and was ignored.

PROPERTIES OF MIXTURES

In this study, C_2H_5OH/Air , C_7H_{16}/Air and C_8H_{18}/Air mixtures were studied at initial pressure of 100kPa. Initial pressure of 325 K was selected to ensure that liquid fuels were completely vaporized before combustion at all equivalence ratios. Equivalence ratio, ϕ , can be calculated by $\phi=3/X_0$, $\phi=11/X_0$, $\phi=12.5/X_0$, respectively, where X_0 are the number of moles of oxygen per one mole of fuel in a mixture. Table 1 shows that the properties of the mixtures used in this study. ρ_b/ρ_u is the ratio of the burned to unburned gas density and T_{ad} is the adiabatic flame temperature calculated by EQUIL code (6), α is the thermal diffusivity, S_u^0 is the unstretched laminar burning velocity obtained experimentally. Le is the Lewis number based on the molecular diffusion coefficient of the deficient reactants. All thermodynamic and transport properties were evaluated by CHEMKIN (6).

Table1 Properties of mixtures

	ϕ	ρ_b/ρ_u	α [mm ² /s]	T_{ad} [K]	S_u^0 [cm/s]	Le
C_2H_5OH/Air ($T_u=325K$)	0.8	0.150	23.50	2051	27.7	1.775
	0.9	0.140	23.24	2177	35.3	1.761
	1.0	0.134	23.00	2256	38.8	1.761
	1.1	0.132	22.74	2254	41.2	1.016
	1.2	0.133	22.50	2188	38.2	1.009
	1.3	0.135	22.25	2116	32.5	1.004
	1.4	0.137	22.02	2040	25.9	0.998
	1.5	0.139	21.82	1973	21.0	0.992
C_7H_{16}/Air ($T_u=325K$)	0.8	0.150	23.54	2074	26.4	3.060
	0.9	0.140	23.30	2208	34.1	3.042
	1.0	0.133	23.08	2292	38.9	3.042
	1.1	0.131	22.85	2294	40.5	1.013
	1.2	0.132	22.63	2224	37.3	1.007
	1.3	0.133	22.43	2153	32.6	1.001
	1.4	0.135	22.21	2078	28.1	0.995
	1.5	0.137	22.01	2001	22.7	0.989
C_8H_{18}/Air ($T_u=325K$)	0.8	0.150	23.51	2071	24.4	3.206
	0.9	0.139	23.28	2205	29.1	3.189
	1.0	0.133	23.05	2289	33.3	3.189
	1.1	0.131	22.82	2290	35.3	1.009
	1.2	0.132	22.60	2209	32.4	1.002
	1.3	0.133	22.39	2150	28.1	0.996
	1.4	0.135	22.17	2072	23.1	0.989
	1.5	0.137	21.97	1995	16.3	0.983

SPHERICALLY PROPAGATING FLAMES

Firstly we investigated the way spherical flames propagate for equivalence ratios ranging from 0.8 to 1.5. Figure 2 plots the results on the flame speeds, dr/dt , as a function of elapsed time from ignition, t , obtained by schlieren images. It is found that dr/dt increases with increasing t for the fuel-lean region, while dr/dt decreases with increasing t for the fuel-rich region. Such way spherical flames propagate is consistent with the previous studies (7)(8) in which this was explained by the interactions between flame stretch and Lewis number effect. That is, the flames having Lewis number less than unity (they are flames on the fuel-rich region, as can be seen in Table 1) propagate faster at the early stage of combustion (at the period of strong flame stretch), then decelerate gradually with time (as flame stretch gets weaker), because flame stretch increases flame speeds for them. On the other hand, flames having Lewis number larger than unity (they are flames on the fuel-lean region, as can be

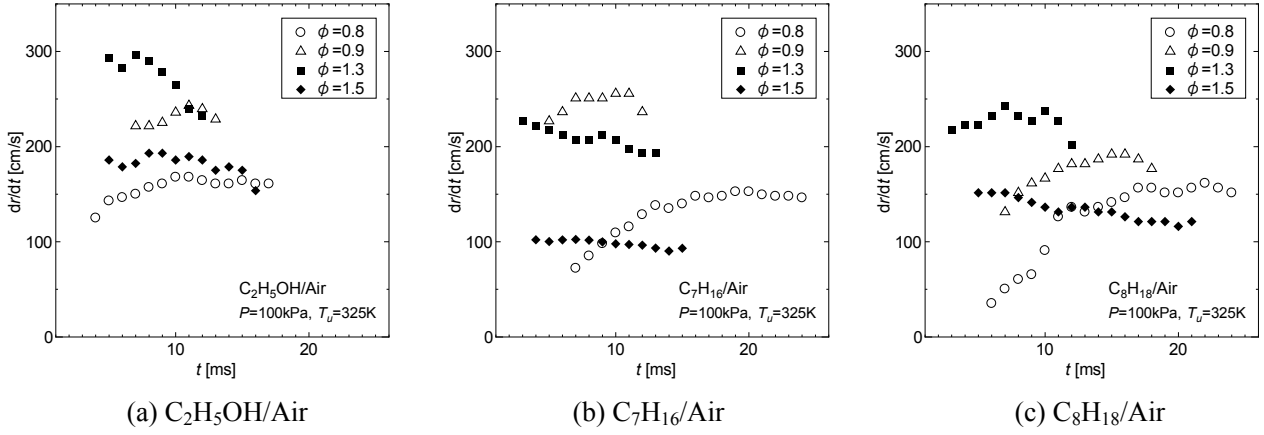


Fig.2 Variations of dr/dt with t

seen in Table 1) propagate slower at the early stage of combustion (at the period of strong flame stretch) then accelerate gradually with time (as flame stretch gets weaker), because flame stretch decreases flame speeds for them.

LAMINAR BURNING VELOCITY

Secondly we investigated the effects of flame stretch on the laminar burning velocities and obtained unstretched laminar burning velocities. As far as the effect of flame stretch on the laminar burning velocities is concerned, they were correlated using an early proposal of Markstein (9), after later generalization and extension at the limit of small stretch as discussed by Clavin (10), as follows.

$$S_u = S_u^0 - L_u \kappa \quad (1)$$

Where L_u , which is referred to as Markstein length, represents the sensitivity of S_u to the stretch rate, κ , for a given mixture. The Markstein length is proportional to a characteristic flame thickness, δ_T^0 , so that a dimensionless Markstein number, Ma , can be defined as:

$$Ma = L_u / \delta_T^0 \quad (2)$$

The stretch rate, κ , can be also non-dimensionalized by characteristic flow time to obtain the Karlovitz number, Ka , as follows.

$$Ka = \kappa / (S_u^0 / \delta_T^0) \quad (3)$$

From Eqs.(1)-(3), the below relationships are derived:

$$\frac{S_u}{S_u^0} = 1 - Ma \times Ka \quad (4)$$

From Eq.(4), it is found that the decrease in the burning velocity of stretched flame becomes relatively smaller with decreasing Ma at the same Karlovitz number.

As far as flame stretch is concerned, it consists of two physical processes (11). The first of these is the tangential strain rate on the flame surface noted by a_{tt} which is often characterized by the local velocity gradients in the reactant just upstream of the flame. The second process is the propagation of a curved flame, and can be characterized by the arithmetic mean of the local principle curvature (h) and local propagation velocity relative to the reactant fluid (S_b). The quantity S_b which is known as the displacement velocity of the flame is the speed of propagation of the flame relative to its center of curvature. The flame stretch when written in terms of strain and curvature is given, by the following exact equation (11).

$$\kappa = a_{tt} + 2S_b h$$

For spherically propagating flames, the laminar burning velocity and flame stretch are given as follows (12),

$$S_u = (\rho_b / \rho_u) dr/dt, \quad \kappa = (2/r) dr/dt$$

The density ratio needed to find S_u was computed assuming adiabatic constant pressure combustion with the same concentrations of elements in the unburned and burned gases.

Figure 3 plots laminar burning velocity, S_u , as a function of flame stretch, κ , for C_7H_{16}/Air with $\phi=1.5$ as example. It is found that relationship between κ and S_u exhibits linearity clearly, as seen in Eq.(1). This holds true for all mixtures used in this study. A linear extrapolation of the S_u values

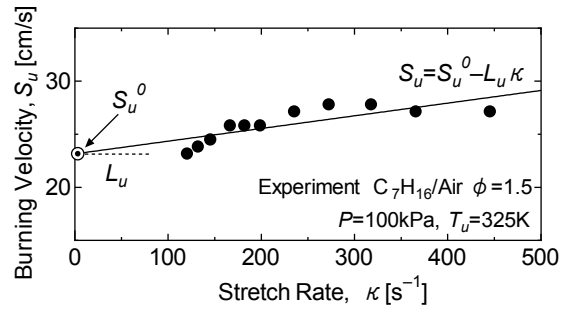


Fig.3 Variation of S_u with κ

to zero stretch rate yields unstretched laminar burning velocity, S_u^0 , and the slope of the results yields Markstein length, L_u , which, in turn, yields Ma by Eq.(2).

Figure 4 plots experimental results of S_u/S_u^0 as a function of Ka , for some specified equivalence ratios. Again the linear relationship between Ka and S_u/S_u^0 can be appreciable. In addition, the behaviour of S_u/S_u^0 is found to depend on the equivalence ratio, ϕ . That is, S_u/S_u^0 decreases with decreasing ϕ (increasing Le , as seen in Table 1) at the same Ka . It should be noted that the slope of these lines corresponds to Markstein number, Ma for each mixture.

Figure 5 (a)(b)(c) show the variation of un-stretched laminar burning velocities, S_u^0 , with ϕ , obtained for C_2H_5OH/Air , C_7H_{16}/Air and C_8H_{18}/Air mixtures, respectively, along with the data obtained by Egolfopulous et al. (2), Gulder (3) and Davis et al. (13).

For ethanol-air flames in Fig.5 (a), there is good agreement between our data and data by Egolfopulous et al. and Gulder for all the equivalence ratios, except for the equivalence ratio

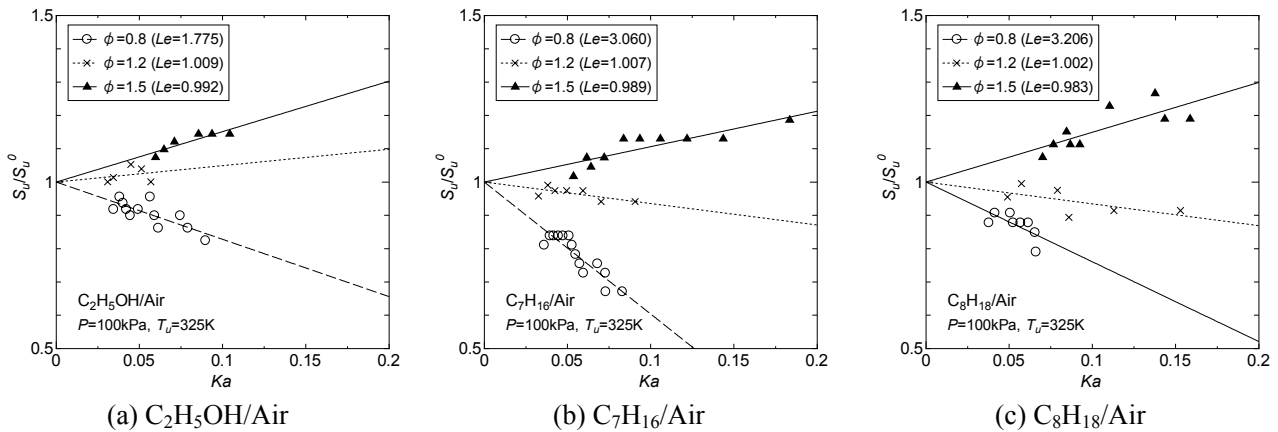


Fig.4 Variations of S_u/S_u^0 with Ka

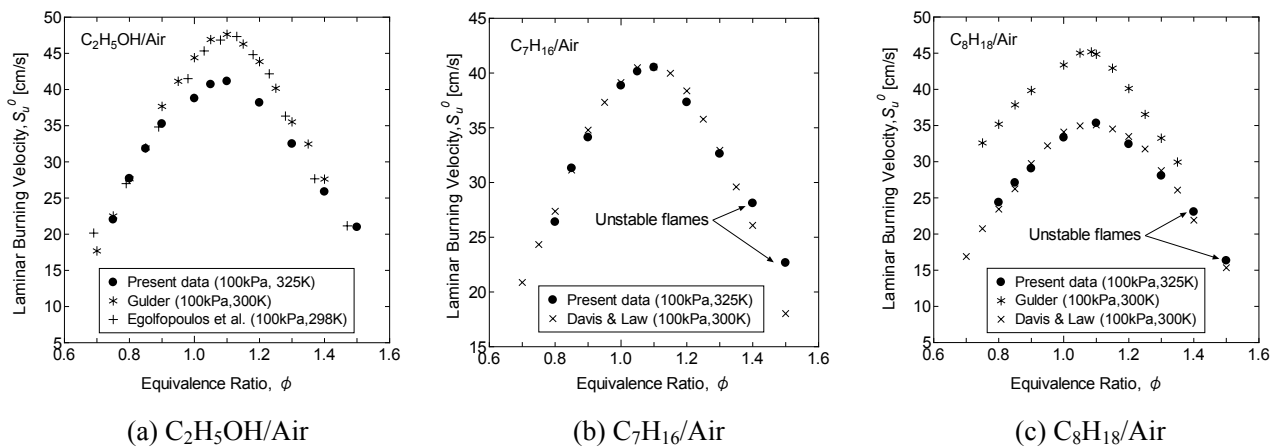


Fig.5 Variations of S_u^0 with ϕ

between 1.0 and 1.2, where our data give smaller values, although our experimental condition has higher initial temperature ($T_u = 325\text{K}$) compared to Egolfopulous et al. ($T_u = 298\text{K}$) and Gulder ($T_u = 300\text{K}$). This could be due to the differences of flame configuration and experimental procedures. Egolfopulous et al. have used counter flame method, which has some ambiguity for the definition of flame position. Gulder has used the same type of combustion bomb as ours, but he has used ionization probes to specify the flame position.

For *n*-heptane-air flames in Fig.5 (b), there is good agreement between our data and data by Davis et al. for all the equivalence ratios. In addition, flame surface of *n*-heptane-air mixtures with $\phi = 1.4$ and 1.5, that initially appear smooth were found to show cellularity later, while flame surfaces of ethanol-air mixtures were found to remain smooth for all equivalence ratios. This behaviour appears to be quite general since at low Markstein number (low Lewis number), all spherically expanding flames are intrinsically unstable, with no stabilizing influence due to thermodiffusive effects. Flame instability has many influences on combustion properties, such as burning velocities. Therefore we discuss in more detail in the next section.

For *iso*-octane-air flames in Fig.5 (c), there is also good agreement between our data and data by Davis et al. for all the equivalence ratios, while data by Gulder give higher vales for all the equivalence ratios. Again, this could be due to the fact that Gulder has used ionization probes to specify the flame position. The flame surface of *iso*-octane-air mixtures with $\phi = 1.4$ and 1.5, were also found to be unstable.

Figure 6 shows the comparison of un-stretched laminar burning velocities of ethanol-air, *n*-heptane-air and *iso*-octane-air flames. In this figure, it is found that ethanol-air and *n*-heptane/air flame have almost the same value of S_u^0 over all the ranges of equivalence ratios, while *iso*-octane/air flames are found to give smaller value of S_u^0 for these regions.

Figure 6 shows the comparison of un-stretched laminar burning velocities of ethanol-air, *n*-heptane-air and *iso*-octane-air flames. In this figure, it is found that ethanol-air and *n*-heptane/air flame have almost the same value of S_u^0 over all the ranges of equivalence ratios, while *iso*-octane/air flames are found to give smaller value of S_u^0 for these regions.

THE EFFECTS OF METHANOL ADDITION ON OCTANE AND HEPTANE FLAMES

Finally, we investigated the effects of ethanol addition to *n*-heptane and *iso*-octane-air flames in terms of flame instability. As flames gets instable, cellular flames triggers. Then the flame surface area increases, which leads to an increase in the burning velocity. This can affect the system performance of an engine. There are two types of instabilities (10). The first is called the hydrodynamic instability and is caused by the density change across a flame. The second instability is due to differential diffusion of reactants and energy, and is called the thermal-diffusive instability. The thermal-diffusive instability occurs when the Lewis number is less than some critical value, which can be realized by changing a kind of fuel.

To quantify the amounts of added ethanol and to investigate the effects of ethanol addition, the volume fraction of the added ethanol in the whole fuel, δ , was defined. In this case, mixture compositions can be expressed as,

$(1-\delta)\text{C}_7\text{H}_{16} + \delta\text{C}_2\text{H}_5\text{OH} + X_0(\text{O}_2 + 3.76\text{N}_2)$ for *n*-heptane-air cases.

$(1-\delta)\text{C}_8\text{H}_{18} + \delta\text{C}_2\text{H}_5\text{OH} + X_0(\text{O}_2 + 3.76\text{N}_2)$ for *iso*-octane-air cases.

In addition, total equivalence ratio, ϕ , was defined by $\phi = (11-8\times\delta)/X_0$, $\phi = (12.5-9.5\times\delta)/X_0$, respectively. We observed the flames using schlieren system varying δ for $\phi = 1.5$, where both solo *n*-heptane-air flame and solo *iso*-octane-air flame ($\delta = 0$) were found to get unstable.

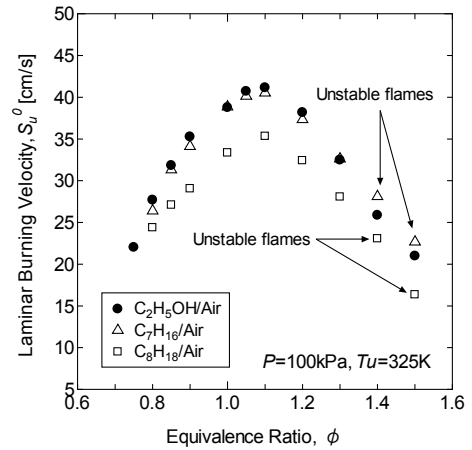


Fig.6 Variation of S_u^0 with ϕ

Acknowledgements

This work was partially supported by Grant-in-Aid for Science Research No.14750143 from the Ministry of Education, Science and Culture of Japan. We would like to thank Mr.Miyahara, Mr. Oda, Mr.Shigeharu and Mr.Okubo for their help with experiment.

NOMENCLATURE

a_{tt}	Tangential strain rate on the flame surface
h	Local principle flame curvature
Ka	Karlovitz number
Le	Lewis number
L_u	Markstein length
Ma	Markstein number
S_u	Stretched laminar burning velocity
S_u^0	Unstretched laminar burning velocity

Greek symbols

α	Thermal diffusivity
δ_T^0	Laminar flame thickness
ϕ	Equivalence ratio
κ	Stretch rate
ρ	Mixture density

Subscript

u	Properties associated with the unburned mixtures
b	Properties associated with the burned mixtures

REFERENCES

- (1) Stiesch, G., "Modelling Engine Spray and Combustion Processes", Springer, 1994.
- (2) Egolfopoulos, F.N., Du, D.X., Law, C.K., "A study on Ethanol oxidation kinetics in laminar premixed flames, flow reactors and shock tubes", Proc. Combust. Inst. 24, pp.833-841, 1992.
- (3) Gulde, O.L., "Laminar burning velocities of methanol, Ethanol and isooctane-air mixtures", Proc. Combust. Inst. 19, pp.275-281, 1982.
- (4) Tanoue, K., et al., "The effects of Flame Stretch on Outwardly Propagating Flames", JSME Int. J. Series B, Vol.46, pp.416-424, 2003.
- (5) Tanoue, K., "Effects of Flame Stretch on Laminar Methane Flames with Hydrogen Addition", Proc. 6th ASME-JSME Thermal Engineering Joint Conference, CD-ROM 2003.
- (6) Kee, R.J., Rupley, F.M. and Miller, J.A. et al., CHEMKIN Collection, Release 3.7, Reaction Design, Inc., San Diego, CA, 2003.
- (7) Tseng, L.-K., Ismail, M.A., and Faeth, G.M., Combust. Flame, Vol.95, pp.410-426, 1993.
- (8) Bradley, D., Gaskell, P.H., and Gu, X.J., Proc. Combust. Inst. 27, pp.849-856, 1998.
- (9) Markstein, G. H., Non-steady Flame Propagation, Pergamon, Oxford, 1964.
- (10) Clavin, P., Prog. Energy Combust. Sci., Vol.11, pp.1-59, 1985.
- (11) Poinso, T., Candel, S. and Trounev, A., "Applications of direct numerical simulation to premixed turbulent combustion", Prog. Energy Combust. Sci., Vol.21, pp.531-576, 1996.
- (12) Law, C.K., and Sung, C.J., "Structure, aerodynamics, and geometry of premixed flamelets", Prog. Energy Combust. Sci., Vol.26, pp.459-505, 2000.
- (13) Davis, S.G. and Law, C.K., "Laminar Flame Speeds and Oxidation Kinetics of iso-Octane-Air and n-Heptane-air Flames", Proc. Combust. Inst. 27, pp.521-527, 1998.